TDOA BASED ROBUST EKF LOCALIZATION FOR LTE

A THESIS

submitted by

ROHAN SRIRAM

for the award of the degree

of

B.TECH AND M.TECH

DEPARTMENT OF ELECTRICAL ENGINEERING
INDIAN INSTITUTE OF TECHNOLOGY MADRAS.

MAY 2014

THESIS CERTIFICATE

This is to certify that the thesis titled **TDoA Based Robust EKF Localization for LTE** , submitted by **Rohan Sriram**, to the Indian Institute of Technology, Madras, for the award of the degree of **B.Tech and M.Tech**, is a bona fide record of the research work done by him under our supervision. The contents of this thesis, in full or in parts, have not been submitted to any other Institute or University for the award of any degree or diploma.

Prof. Devendra Jalihal
Research Guide
Professor
Dept. of Electrical Engineering
IIT-Madras, 600 036

Place: Chennai

Date: 15th May 2014

ACKNOWLEDGEMENTS

This thesis is a culmination of my five years stay at the Indian Institute of Technology Madras. I experienced a number of highs and lows over this time and met a number of people who have inspired and influenced me to make me the person I am today. I am unlikely to do full justice to this list of people, but here goes. I would like to thank Prof. Devendra Jalihal for guiding me along the right direction whenever I was stuck, my family for always reminding me I can do better. I'd like to thank Swarun and rest of the Saras gang for their good natured fun, countless football discussions and the many mug sessions we had before exams. Thanks to Gokul and Vichy, my school friends for all the fun holidays we had over these years. To Sujan and Avantika who were there for me when I was "growing" up. To the so called "rebel" elec gang for all the fun we had in and out of classes. To Barathan, Terror, Sai and Tiru for good times in the hostel and to Deva who's crazy fitness obsession pushed me to train harder. To Sohini, Girish and GV for the all the wonderful times in the department. To Navneeth, the rest of the core team and my team of coordinators who helped pull off one of the more memorable "Evolves" in Shaastra. To the Tapti cricket team with whom we shared highs like winning Gold in Schroeter and rock bottom lows. And finally, a shout out to all those others who I have interacted with and who have left their own special mark on me. Thank you.

ABSTRACT

KEYWORDS: LTE Positioning, TDoA, Adaptive Kalman Filter

With the advent of location based services, the need for accurate positioning of mobile stations has been growing. Global Positioning Systems (GPS) using satellites can deliver very good estimates of position under certain conditions. However in urban and indoor areas, positioning with GPS is almost impossible. The new cellular wireless communication systems, like the OFDM based 3GPP-LTE, provide excellent coverage in urban and most indoor environments . One of the techniques used in position estimation is Kalman Filtering using Time Difference of Arrival (TDoA) measurements of the 3GPP-LTE signals. However, this approach assumes the knowledge of the mobility model and statistics of the Mobile Station (MS). To overcome this, we propose an adaptive Kalman filter algorithm for localization which does not assume any information about the statistics of the MS mobility model. First we develop an error model for Time of Arrival (ToA) and Time Difference of Arrival (TDoA) under certain typical scenarios. We then present our algorithm and evaluate the performance of the algorithm under these different scenarios.

TABLE OF CONTENTS

LIST OF TABLES

LIST OF FIGURES

ABBREVIATIONS

AoA	Angle of Arrival
AoD	Angle of Departure
BS	Base Station
CID	Cell Identification
E-CID	Enhanced-CID
EKF	Extended Kalman Filter
FP	First Path
GLoS	Geometric Line of Sight
GPS	Global Positioning Systems
H.O.T.	Higher Order Terms
ITU	International Telecommunication Union
KDE	Kernel Density Estimation
LTE	Long Term Evolution
MS	Mobile Station
NLoS	Non-Line of Sight
OTDoA	Observed Time Difference of Arrival
OFDM	Orthogonal Frequency Division Multiplexing
PRS	Position Reference Signal
RSS	Received Signal Strength
RSSI	Received Signal Strength Indicator
RSTD	Reference Signal Time Difference
SP	Strongest Path
ToA	Time of Arrival
TDoA	Time Difference of Arival
UE	User Equipment

CHAPTER 1

INTRODUCTION

Services and applications based on accurate knowledge of user position, such as location-sensitive billing, fraud detection, recommendation systems based on location etc have become more and more prominent. These location requirements can be met by global navigation satellite systems. However in some environments, the GPS signals may be too weak to detect or much too scattered to provide required accuracy.(Gentner *et al.*, 2012) Several methods are available to provide good coverage in GPS critical environment, eg. cell identification (CID), received signal strength (RSS), angle of arrival (AoA), time of arrival (ToA) and time difference of arrival (TDoA). The LTE standard has provided support for localization. One such method is the Enhanced Cell ID (E-CID) . Another UE-assisted method is the observed time-difference of arrival (OTDoA). In 3GPP-LTE Rel.9, the positioning reference signal (PRS) is introduced to enhance the positioning measurements in combination with low interference subframes, to ensure sufficiently high signal quality and detection probability. The reference signal PRS is used by the UE to measure the time-difference of arrival, which is referred to as RSTD (Reference Signal Time Difference). (del Peral-Rosado *et al.*, 2012).

In this thesis we focus on developing a Kalman based approach to solving the localization problem using RSTD. This type of algorithms as in (Klee *et al.*, 2006) and (Nájar and Vidal, 2001) assumes certain statistics of the mobility of the mobile station. However in practice, such information may not be available. We overcome this problem by developing an adaptive Kalman filter algorithm which assumes no knowledge of the mobile station's mobility. We then demonstrate that even without knowledge of the mobile station's mobility model, this algorithm can deliver better results than a static positioning algorithm.

This thesis is organised as follows. In the next chapter we introduce ToA and TDoA and explain how they can be used to find a position estimate. We then develop an error model for ToA and TDoA under certain typical scenarios encountered in the LTE envrironment. Chapter III gives an overview of Kalman filter and its approach to localization algorithms. In Chapter IV, we present our algorithm and evaluate its performance.

CHAPTER 2

ToA and TDoA: Introduction and Error Models

The key idea behind most localization algorithms is trilateration. It is a method to determine the position of an object based on simultaneous range measurements from three or more known non-collinear locations. For example, in two dimension space, if a point lies on the boundary of two circles simultaneously, then the circle centres and the two radii provide sufficient information to narrow the possible locations down to two. Additional information can narrow the possibilities down to a unique location.

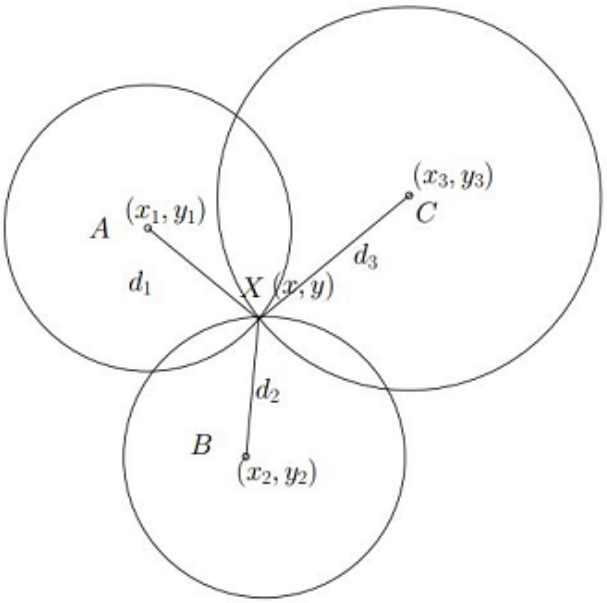

Figure 2.1: Trilateration

Another idea is multi-lateration, which is a technique based on the difference in distances to two or more stations at known locations that broadcast signals at known times. Difference in distances gives us a hyperbolic locus under 2D geometry. Two such measurements results in two curves which intersect giving a small number of possible locations. Some common metrics associated with the localization process are Time of Arrival (ToA), Time Difference of Arrival (TDoA), Angle of Arrival (AoA) and RSSI (Received Signal Strength Indicator). We will concern ourselves only with the first two metrics in this thesis.

2.1 Preliminaries

2.1.1 Definitions

ToA: This measurement refers to the time taken for a radio signal to travel from a transmitter to a receiver. Using this measurement and with the knowledge of speed of light in the medium of propagation, we can calculate the distance between the transmitter and the receiver. Three or more such measurements can be used to do localization by trilateration or multi-lateration.

TDoA: A TDoA measurement refers to the difference in travel times of a radio signal from two distinct transmitters to a single receiver. This can then be used to do localization by muti-lateration.

2.1.2 ToA and TDoA Errors

In Non-Line of Sight (NLoS) environments, the ToA errors may be caused by NLoS effect, presence of multi-path components and/or synchronization strategies. In this work, we focus exclusively on ToA and TDoA errors as a result of multi-path and NLoS scenario. We define the ToA error of a path as the time difference of the path and the Geometric Line of Sight (GLos) path.

As pointed out by (Wang *et al.*, 2009), in geolocations the First Path (FP) and the Strongest Path(SP) attract the most attention. The FP is closest to the GLoS, whereas the SP is the most easiest to be detect or extract from the channel profiles. We can therefore view FP ToA error as a lower bound on the signal's ToA error and the ToA error of SP as indicative of the upper bound on the ToA error. The ToA error of the FP is given by

$$\varepsilon_{ToA_1}^{FP} = \varepsilon_1^{FP} = ToA_1^{FP} - ToA_1^{GLoS} \tag{2.1}$$

where ToA_1^{FP} is the arriving time of the first peak, ToA_1^{GLoS} is the arriving time of the GLoS, and the subscript number $'1'$ stands for the index of the channel from transmitter to receiver. Similarly, the ToA error of SP is defined.

$$\varepsilon_{ToA_1}^{SP} = \varepsilon_1^{SP} = ToA_1^{SP} - ToA_1^{GLoS} \tag{2.2}$$

If another transmitter is taken into account, the TDoA error can be derived for FP and SP respectively as

$$\varepsilon^{FP}_{TDoA_{21}} = (ToA^{FP}_2 - ToA^{FP}_1) - (ToA^{GLoS}_2 - ToA^{GLoS}_1) = \varepsilon^{FP}_{ToA_2} - \varepsilon^{FP}_{ToA_1} \quad (2.3)$$

$$\varepsilon^{SP}_{TDoA_{21}} = (ToA^{SP}_2 - ToA^{SP}_1) - (ToA^{GLoS}_2 - ToA^{GLoS}_1) = \varepsilon^{SP}_{ToA_2} - \varepsilon^{SP}_{ToA_1} \quad (2.4)$$

2.2 Methodology

We study the ToA and TDoA errors under different channel conditions mentioned in the WINNER Phase II channel models using code in (L. Hentila and Alatossava, 2007) and also under the extended ITU Pedestrian B and Vehicular Channel A from (Sørensen and Frederiksen, 2005). We build ToA error models for B1, B2, C1 and C3 scenario of the WINNER channel specifications and for the Extended ITU Ped B and Veh A channel.

2.2.1 Simulation under WINNER package

The WINNER channel models are chosen because their higher complexity provides more flexibility on the simulation test. These models increase the number of paths (i.e. up to 20 paths) leading to rich power delay profiles that can help us assess different situations. The WINNER package describes several channel scenarios. Depending on the scenario selected, large-scale parameters, such as delay spread, angle spread or shadow fading, are randomly generated. The small-scale parameters such as delay, power, AoA and AoD are randomly distributed for each cluster of propagation rays (i.e. rays with similar delay and directions). Finally, the channel realisations are generated according to the random initial phases of the scatterers.(del Peral-Rosado *et al.*, 2012)

The simulation is simplified to a single link between transmitter and receiver with single isotropic antennas. For each scenario, we generate numerous channel realisations with different BS position and MS position and velocity. For each such realisation, the ToA error of the first non-LoS path relative to the GLoS path is noted. Similarly the ToA error of the strongest path is observed. An assumption we make here is that we have perfect knowledge of the position of FP and SP and the relative strengths of each path. We make this assumption because our purpose here is to study the ToA and TDoA

errors under various channel conditions purely due to geometry and not due to errors introduced by the receiver.

The code in (L. Hentila and Alatossava, 2007) exposes the interfaces required to do the above mentioned simulations for each scenario. We obtained 40000 channel realisations for each scenario with BS-MS distances varying from approximately 50m to 600m. For the relative strength of each path, we include the effects of path loss and shadowing.

2.2.2 Simulation for Extended ITU Ped B and Veh A

We use the Extended ITU Vehicular A and Pedestrian B channel listed in (Sørensen and Frederiksen, 2005).We study the tap delay distribution by adding an artificial Gaussian-distributed delay to the fixed tap delay positions. This does not intend to model a realistic variation of the taps delays, but to assess the impact of the delay variation statistically. We define the tap delay variations $\tau_k(j)$ as

$$\tau_k(j) \sim N(\overline{\tau}_k, \sigma_T^2) \tag{2.5}$$

where j is the channel realisation, $\overline{\tau}_k$ is the mean tap delay defined by the channel model, and σ_T is the standard deviation of the artificial delays. We use a standard deviation $\sigma_T = 20$m. Under this, like the previous case we generate 40000 realisations of the channel and fit a probability distribution for FP and SP ToA error. This is done separately for the Ped B and Veh A channel

2.3 ToA Error Models

We now present the ToA error models for FP and SP for each of the above channel scenarios. After fitting a distribution, we use a quantile-quantile plot to view how good our model approximates the sample data.

2.3.1 B1 Scenario - Urban Micro Cell

In urban micro-cell scenarios the height of both the antenna at the BS and at the MS is assumed to be well below the tops of surrounding buildings. Both antennas are assumed to be outdoors in an area where streets are laid out in a Manhattan-like grid. The streets in the coverage area are classified as 'the main street', where there is the LOS from all locations to the BS, with the possible exception in cases where the LOS is temporarily blocked by traffic (e.g. trucks and busses) on the street. Streets that intersect the main street are referred to as perpendicular streets, and those that run parallel to it are referred to as parallel streets. This scenario is defined for both the LOS and the NLOS cases. Cell shapes are defined by the surrounding buildings, and energy reaches NLOS streets as a result of the propagation around corners, through buildings, and between them.(L. Hentila and Alatossava, 2007)

Table 2.1: B1 Scenario: Statistical parameters of ToA Error

$Case$	$Distribution$	$Parameters$	$Mean(m)$	$StandardDeviation(m)$
FP	Weibull	$\lambda = 13.51, k = 0.92$	14.06	15.31
SP	Weibull	$\lambda = 23.32, k = 0.98$	23.55	24.11

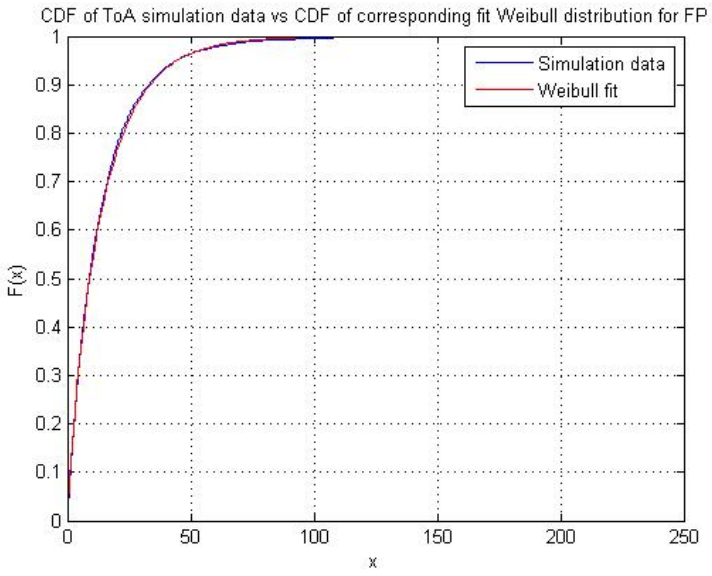

Figure 2.2: B1 Scenario: CDF of FP and corresponding Weibull fit

An insight to the match between ToA error and our fit Weibull distribution is promised by the quantile-quantile plot, which shows the similarity of two distributions. The

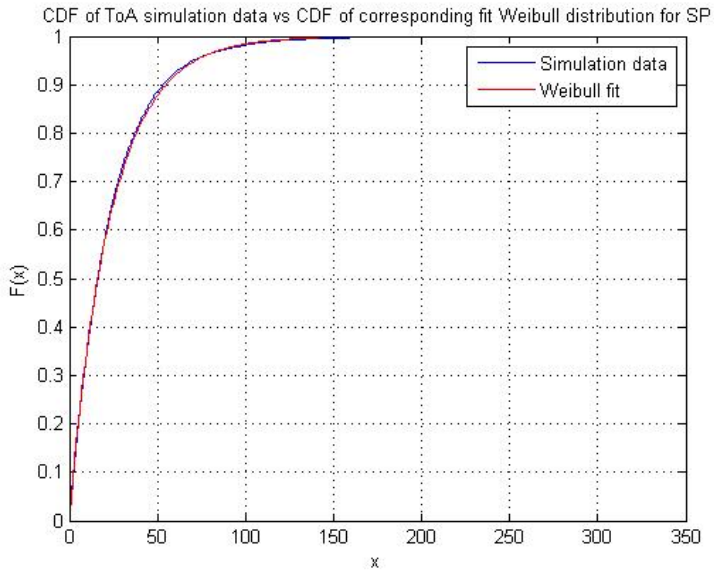

Figure 2.3: B1 Scenario: CDF of SP and corresponding Weibull fit

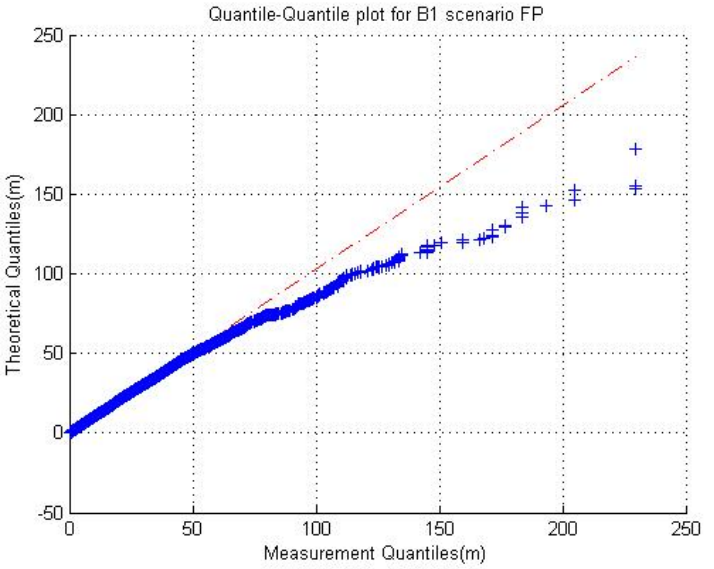

Figure 2.4: B1 Scenario: Quantile-Quantile plot of FP ToA error vs the fit Weibull distribution

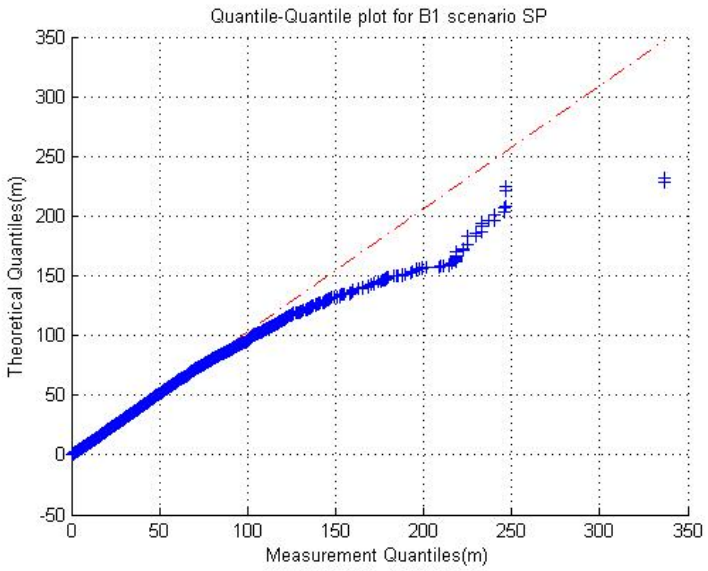

Figure 2.5: B1 Scenario: Quantile-Quantile plot of SP ToA error vs the fit Weibull distribution

quantile-quantile plot is a comparison between two statistic sets. The linearity of the samples in the plot determines the similarity of two distributions. In other words, if two serials of samples have the same distribution, even with different means and variances, the samples should locate in a straight line. Fig.2.4 presents the quantile-quantile plot for the ToA error of FP with respect to our fit Weibull distribution. The y axis represents the theoretical quantiles from the distribution, and the x axis gives the quantiles of the measured data. However, the tail at the right move below the line, which indicates the unsimilarity between the model and the measured data. Apparently our Weibull distribution could model the ToA error of FP except for the tail with low probabilities. In other words, the model will generate smaller ToA errors than the true levels as they are. Similarly Fig. 2.5 shows the corresponding plot for SP.

2.3.2 Extended ITU Ped B Channel

Table 2.2: Extended ITU Ped B: Statistical parameters of ToA Error

$Case$	$Distribution$	$Parameters$	$Mean(m)$	$StandardDeviation(m)$
FP	Nakagami	$\mu = 0.58, \omega = 396.23$	16.31	11.4
SP	Kernel Density	Kernel=Normal, BW $= 4.25$	49.44	28.9

The quantile-quantile plot of our Nakagami fit for ToA error as seen in Fig.2.8 and

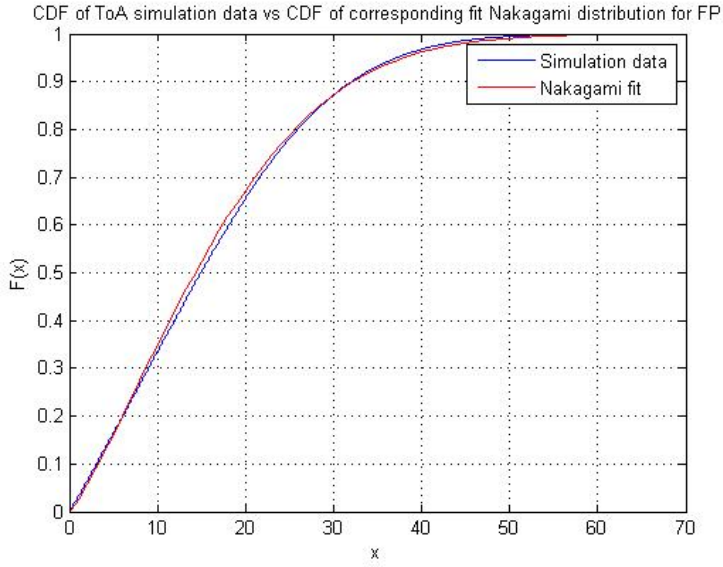

Figure 2.6: Ex ITU Ped B: CDF of FP and corresponding Weibull fit

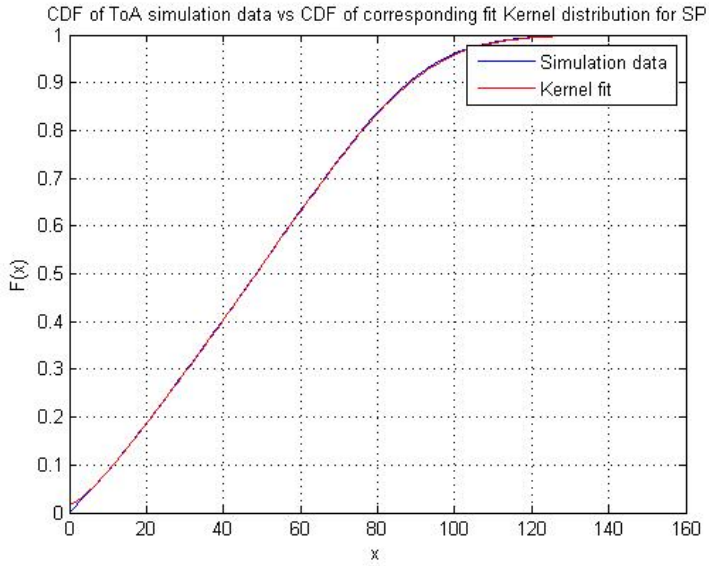

Figure 2.7: Ex ITU Ped B: CDF of SP and corresponding Kernel distribution fit

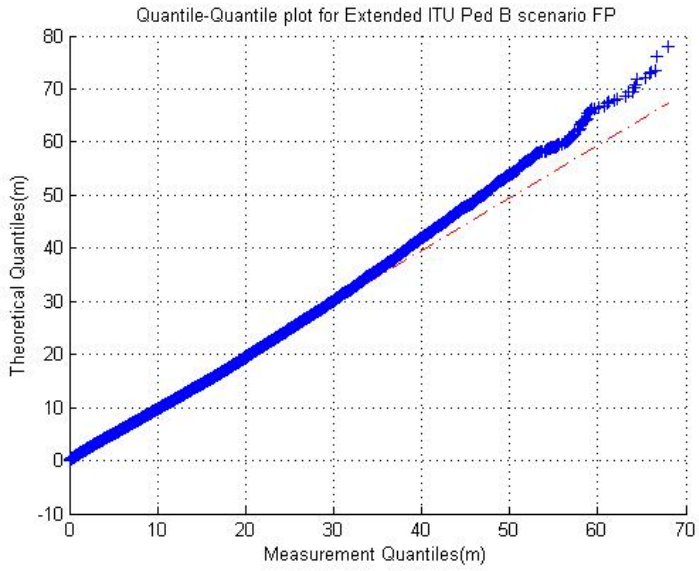

Figure 2.8: Ex ITU Ped B: Quantile-Quantile plot of FP ToA error vs the fit Weibull distribution

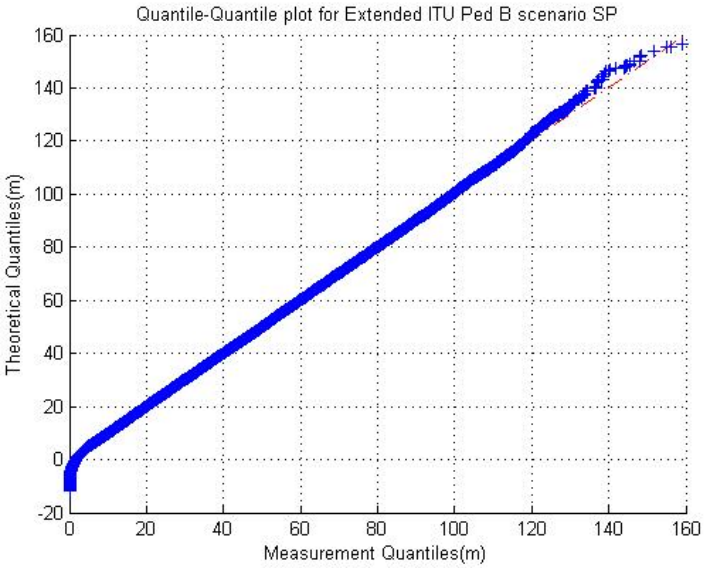

Figure 2.9: Ex ITU Ped B: Quantile-Quantile plot of SP ToA error vs the fit Kernel distribution

KDE fit for SP as seen in Fig. 2.9 suggests that the fit is excellent except possibly for a few outliers.

2.3.3 Extended ITU Veh A Channel

Table 2.3: Extended ITU Ped B: Statistical parameters of ToA Error

$Case$	$Distribution$	$Parameters$	$Mean(m)$	$StandardDeviation(m)$
FP	Nakagami	$\mu = 0.58, \omega = 471.1$	17.77	155.34
SP	Kernel Density	Kernel=Normal, BW $= 6.76$	66.15	41.22

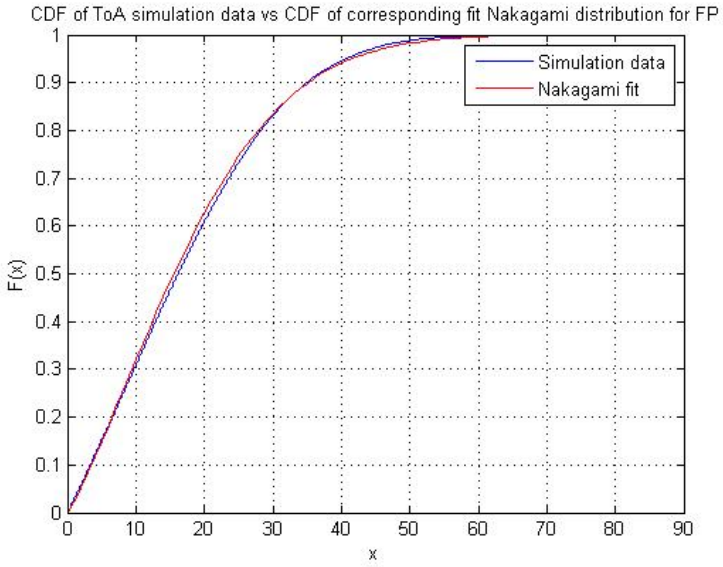

Figure 2.10: Ex ITU Veh A: CDF of FP and corresponding Weibull fit

The quantile-quantile plot of our Nakagami fit for ToA error as seen in Fig.2.12 and KDE fit for SP as seen in Fig. 2.13 suggests that the fit is excellent except possibly for a few outliers.

2.3.4 Other scenarios

We repeat the similar procedure for the B2, C1 and C3 scenario as mentioned by WINNER. We present the results here

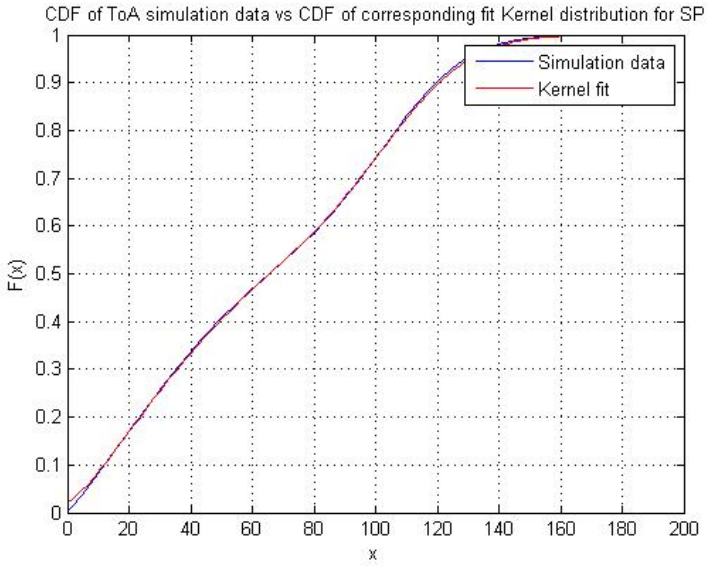

Figure 2.11: Ex ITU Veh A: CDF of SP and corresponding Kernel distributionl fit

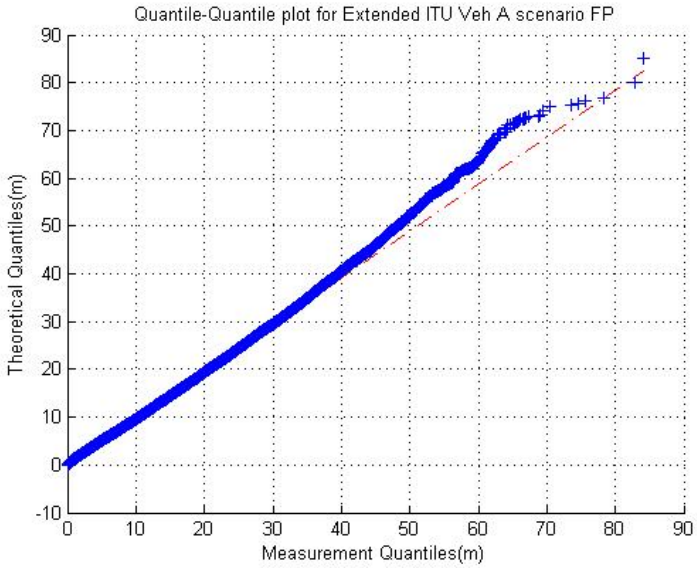

Figure 2.12: Ex ITU Veh A: Quantile-Quantile plot of FP ToA error vs the fit Weibull distribution

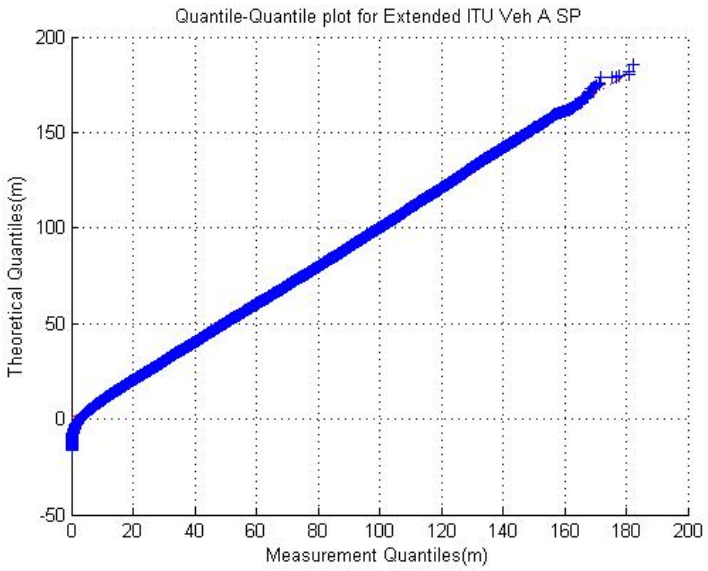

Figure 2.13: Ex ITU Veh A: Quantile-Quantile plot of SP ToA error vs the fit Kernell distribution

B2 Scenario:Bad Urban Macro Cell

Bad urban micro-cell scenarios are identical in layout to Urban Micro-cell scenarios, as described above. However, propagation characteristics are such that multipath energy from distant objects can be received at some locations. This energy can be clustered or distinct, has significant power (up to within a few dB of the earliest received energy), and exhibits long excess delays. Such situations typically occur when there are clear radio paths across open areas, such as large squares, parks or bodies of water.

Table 2.4: B2 Scenario: Statistical parameters of ToA Error

$Case$	$Distribution$	$Parameters$	$Mean(m)$	$StandardDeviation(m)$
FP	Weibull	$\lambda = 14.36, k = 1.03$	14.16	13.7
SP	Weibull	$\lambda = 115.38, k = 1.38$	105.4	77.26

C1 Scenario: Suburban

In suburban macro-cells base stations are located well above the rooftops to allow wide area coverage, and mobile stations are outdoors at street level. Buildings are typically low residential detached houses with one or two floors, or blocks of flats with a few floors. Occasional open areas such as parks or playgrounds between the houses make

the environment rather open. Streets do not form urban-like regular strict grid structure. Vegetation is modest.

Table 2.5: C1 Scenario: Statistical parameters of ToA Error

$Case$	$Distribution$	$Parameters$	$Mean(m)$	$StandardDeviation(m)$
FP	Weibull	$\lambda = 11.00, k = 0.71$	13.69	19.61
SP	Weibull	$\lambda = 38.15, k = 0.73$	46.65	65.38

C3 Scenario: Bad Urban Macro Cell

Bad urban environment describes cities with buildings with distinctly inhomogeneous heights or densities, and results to a clearly dispersive propagation environment in delay and angular domain. The inhomogeneties in city structure can be e.g. due to large water areas separating the built-up areas, or the high-rise skyscrapers in otherwise typical urban environment. Increased delay and angular dispersion can also be caused by mountains surrounding the city. Base station is typically located above the average rooftop level, but within its coverage range there can also be several high-rise buildings exceeding the base station height. From modelling point of view this differs from typical urban macro-cell by an additional far scatterer cluster.

Table 2.6: C3 Scenario: Statistical parameters of ToA Error

$Case$	$Distribution$	$Parameters$	$Mean(m)$	$StandardDeviation(m)$
FP	Weibull	$\lambda = 9.64, k = 0.89$	10.18	11.42
SP	Weibull	$\lambda = 47.96, k = 0.79$	54.56	69.2

2.4 TDoA Error Models

The LTE framework, as mentioned early provides support for localization through TDoA. Hence for the next part of this thesis, which involves localization under LTE, we develop appropriate TDoA error models using the above ToA error models. We attempt to closely approximate TDoA error through a Gaussian Distribution because the Kalman filter algorithm assumes Gaussian noise models. We consider a three BS layout

where TDoA is measured with respect to one common BS. Therefore using equation (2.3), we write (2.6) and (2.7). It can be seen clearly that the two TDoA error values are correlated. We intend to capture this correlation by fitting a multidimensional Gaussian distribution.

$$\varepsilon^{FP}_{TDoA_{21}} = \varepsilon^{FP}_{ToA_2} - \varepsilon^{FP}_{ToA_1} \tag{2.6}$$

$$\varepsilon^{FP}_{TDoA_{31}} = \varepsilon^{FP}_{ToA_3} - \varepsilon^{FP}_{ToA_1} \tag{2.7}$$

A two dimensional Gaussian distribution fit on $\varepsilon^{FP}_{TDoA_{21}}$ and $\varepsilon^{FP}_{TDoA_{31}}$ will give us a covariance matrix which will give us the correlation between the two variables and also the variance of each individually.

Given two independent random processes $a1$ and $a2$ from the same distribution with mean μ and standard deviation σ, their subtraction will be a zero mean process with the standard deviation of $\sqrt{2}\sigma$, which approximately holds for the ToA error and TDoA error models we have developed.

Note: We only do this exercise for the B1 scenario, Extended ITU Ped B and Veh A channels. This is because these three scenarios are the ones we use to test our localization algorithms. Similar models can be built for the other channel scenarios and used for testing the localization algorithms but in this thesis we restrict ourselves to these three scenarios.

2.4.1 B1 Scenario: Urban Microcell

The covariance column in table 2.7 gives the covariance between $\varepsilon^{FP}_{TDoA_{21}}$ and $\varepsilon^{FP}_{TDoA_{31}}$ as per equations (2.6) and (2.7). The mean column refers to the mean of $\varepsilon^{FP}_{TDoA_{21}}$ or $\varepsilon^{FP}_{TDoA_{31}}$ as they are identically distributed. Similarly the standard deviation column refers to the standard deviation of $\varepsilon^{FP}_{TDoA_{21}}$ or $\varepsilon^{FP}_{TDoA_{31}}$

Table 2.7: B1 Scenario: Gaussian statistical parameters of TDoA Error

$Case$	$Mean(m)$	$StandardDeviation(m)$	$Covariance(m^2)$
FP	0	21.61	229.7
SP	0	34.37	600.4

Fig. 2.14 shows the joint probability density function of $\varepsilon^{FP}_{TDoA_{21}}$ and $\varepsilon^{FP}_{TDoA_{31}}$ using the Gaussian distribution described in table 2.7

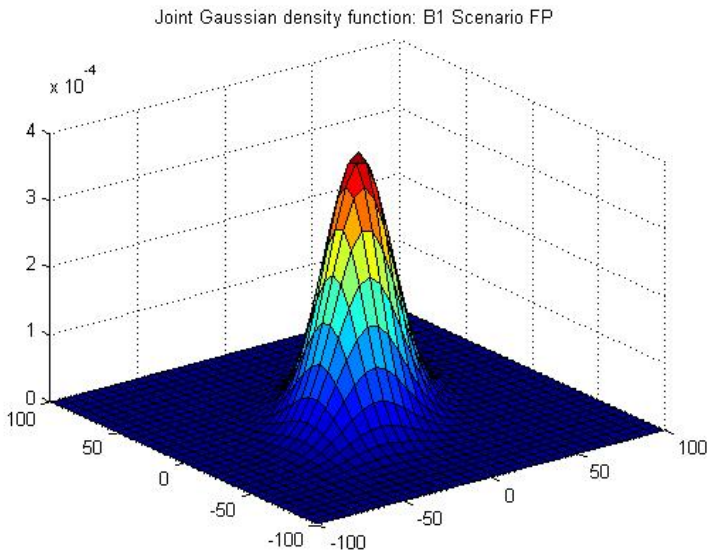

Figure 2.14: B1 Scenario: Joint probability density function based on Gaussian model of FP in table 2.7

2.4.2 Extended ITU Ped B Channel

Similar to the above B1 case, we develop a Gaussian model for TDoA error under this scenario

Table 2.8: Extended ITU Ped B: Gaussian statistical parameters of TDoA Error

$Case$	$Mean(m)$	$StandardDeviation(m)$	$Covariance(m^2)$
FP	0	16.23	133.55
SP	0	40.72	813.9

2.4.3 Extended ITU Veh A Channel

Table 2.9 gives the parameters of the Gaussian distribution under this scenario

Table 2.9: Extended ITU Veh A: Gaussian statistical parameters of TDoA Error

$Case$	$Mean(m)$	$StandardDeviation(m)$	$Covariance(m^2)$
FP	0	17.54	153.44
SP	0	58.55	1715.3

2.5 Final Remarks

The ToA and TDoA error models we have developed above play an important role in defining the environment in which we carry tests for our localization algorithms. We use these models to obtain ToA error values as seen by the MS. The TDoA joint Gaussian model is used as the noise covariance matrix in positioning algorithms.

CHAPTER 3

Introduction to Kalman Filter and Application in Localization

The Kalman filter is an algorithm that uses a series of measurements observed over time, containing noise to produce estimates of unknown variables that tend to be more precise than those based on a single measurement alone. The Kalman Filter uses a state transition model and a set of sequential measurements to produce an estimate of the system's state sequence. It was originally developed as a linear filter but can be extended to non-linear scenarios. We now give a mathematical formulation of the Extended Kalman Filter. See (Terejanu)

3.1 Model Formulation and Assumptions

Consider the following non-linear system described by the difference equation and the observation model with additive noise.

$$x_k = f(x_{k-1}) + w_{k-1} \tag{3.1}$$

$$z_k = h(x_k) + v_k \tag{3.2}$$

The initial state x_0 is a random vector with known mean $\mu_0 = E[x_0]$ and covariance $P_0 = E[(x_0 - \mu_0)(x_0 - \mu_0)^T]$. We assume that the random vector w_k captures uncertainities in the model and v_k denotes the measurement noise. Both are temporally uncorrelated (white noise), zero-mean random sequences with known covariances, and both of them are uncorrelated with the initial state x_0.

$$E[w_k] = 0 \quad E[w_k w_k^T] = Q_k \quad E[w_k w_j^T] = 0 \, for \, k \neq j \quad E[w_k x_0^T] = 0 \, for \, all \, k \tag{3.3}$$

$$E[v_k] = 0 \quad E[v_k v_k^T] = Q_k \quad E[v_k v_j^T] = 0 \, for \, k \neq j \quad E[v_k x_0^T] = 0 \, for \, all \, k \tag{3.4}$$

Also the two vectors w_k and v_k are uncorrelated

$$E[w_k v_j^T] = 0 \, for \, all \, k \, and \, j \tag{3.5}$$

Vectorial functions $f(.)$ and $(.)$ are assumed to be C^1 functions (the function and it's first derivative are continuous on the given domain)

Dimension and Description of variables

x_k $n \times 1$ - State Vector

w_k $n \times 1$ - Process Noise Vector

z_k $m \times 1$ - Observation Vector

v_k $m \times 1$ - Measurement Noise Vector

$f(.)$ $n \times 1$ - Process Vector function

$h(.)$ $m \times 1$ - Observation Vector function

Q_k $n \times n$ - Process Noise Covariance Matrix

R_k $n \times 1$ - Measurement Noise Covariance Matrix

3.2 Extended Kalman Filter Algorithm

Here we present the stages of the EKF as per the model defined in section 3.1

Initialization:

$x_0^a = \mu_0$ with error covariance P_0

Model Forecast Step/Predictor:

$x_k^f \approx f(x_{k-1}^a)$

$P_k^f = J_f(x_{k-1}^a) P_{k-1} J_f^T(x_{k-1}^a) + Q_{k-1}$

Data Assimilation Step/Corrector:

$x_k^a = x_k^f + K_k(z_k - h(x_k^f))$

$K_k = P_k^f J_h^T(x_k^f) \left(J_h(x_k^f) P_k^f J_h^T(x_k^f) + R_k \right)^{-1}$

$P_k = \left(I - K_k J_h(x_k^f) \right) P_k^f$

where J_f is the Jacobian of $f(.)$ and J_h is the Jacobian of $h(.)$

3.3 Application in Localization

3.3.1 Existing Method

As discussed in (Nájar and Vidal, 2001), the use of the Kalman filter allows tracking the position and speed of the UE, yielding an accurate location prediction algorithm. The state transition equation is defined as

$$s(k+1) = As(k) + w(k) \tag{3.6}$$

where $s(k) = [x(k), y(k), v_x(k), v_y(k)]^T$ is the dynamic state vector, where its components represent the UE position and its speed in two-dimensional Cartesian coordinates at discrete times k. The matrix A is the state matrix with Δ equal to the time interval between samples

$$A = \begin{bmatrix} 1 & 0 & \Delta & 0 \\ 0 & 1 & 0 & \Delta \\ 0 & 0 & 1 & 0 \\ 0 & 0 & 0 & 1 \end{bmatrix} \tag{3.7}$$

and $w(k) = [0, 0, w_x(k), w_y(k)]^T$ is the disturbance transition vector defined as a two dimensional random speed vector with covariance Q.

The observation equation is defined as (Assuming a 3 BS Scenario)

$$z(k) = h(s(k)) + v(k) \tag{3.8}$$

where $z(k) = [TDoA_{21}, TDoA_{31}]^T$ represents the actual TDoA values of the MS-BS system, $h(.)$ is the non-linear function that calculates the theoretical geometric TDoA values from $s(k)$.

$$h(s(k)) = \begin{bmatrix} \sqrt{(x(k) - x_{BS_2})^2 + (y(k) - y_{BS_2})^2} - \sqrt{(x(k) - x_{BS_1})^2 + (y(k) - y_{BS_1})^2} \\ \sqrt{(x(k) - x_{BS_3})^2 + (y(k) - y_{BS_3})^2} - \sqrt{(x(k) - x_{BS_1})^2 + (y(k) - y_{BS_1})^2} \end{bmatrix} / c \tag{3.9}$$

where x_{BS_j} and y_{BS_j} represents the position of BS j in a coordinate system where $x(k)$ and $y(k)$

represents the position of MS, c is the speed of light and $v(k)$ is the noise term which captures errors in TDoA with covariance R.

Now once the model has been set up, we can run the Extended Kalman Filter as and when measurements are obtained to estimate the position of the MS at each instant.

3.3.2 Problem Statement

In the above method, we assume the knowledge of the statistics of the disturbance transition vector $w(k)$ and the statistics of the TDoA noise vector $v(k)$. Also taken for granted is the correctness of the model as defined by equation (3.1). As discussed in the previous chapter, it may be possible to model the statistics of the TDoA noise vector but the statistics of the disturbance transition vector is not easy to obtain. The covariance of $w(k)$ depends on the acceleration of the MS which itself might be varying in an unknown fashion.

We therefore propose an alternate formulation of this localization problem and develop an adaptive Kalman filter algorithm which does not assume the knowledge of the statistics of $w(k)$ and $v(k)$.

Alternate Formulation of Existing Localization Problem

There are two ways we tackle the problem mentioned above. The first approach is to retain the state and observation equations discussed under subsection 3.3.1 and run our developed adaptive Kalman Filter algorithm on this model.**Note:** This formulation differs from the one under subsection 3.3.1 by the fact that we do not know the statistics of $w(k)$ and $v(k)$.

However there is a second approach. Since our TDoA measurements are explicit measurements of $x(k)$ and $y(k)$, using $v_x(k)$ and $v_y(k)$ in the state description seems superfluous. We instead use a state transition equation as shown in equation (3.10).

$$s(k+1) = As(k) + w(k) \tag{3.10}$$

where $s(k) = [x(k), y(k)]^T$ is the dynamic state vector, where its components represent

the UE position in two-dimensional Cartesian coordinates at discrete times k. The matrix A is the state matrix

$$A = \begin{bmatrix} 1 & 0 \\ 0 & 1 \end{bmatrix} \tag{3.11}$$

and $w(k) = [w_x(k), w_y(k)]^T$ is the disturbance transition vector defined as a two dimensional random position vector with unknown covariance Q. We retain the same observation equation as under 3.3.1. The $v_x(k)\Delta$ and $v_y(k)\Delta$ are subsumed in $w(k)$.

This model is equivalent to saying that the MS at every step can be found in a region around its previous position. Under this new formulation we test our adaptive Kalman Filter algorithm.

Important: Our adaptive Kalman filter algorithm has been tested under both formulations and gives identical results. However in this thesis, we present the results as obtained under the second formulation

CHAPTER 4

Adaptive Kalman Filter Algorithm for Localization

4.1 Preliminaries

We propose to use an Adaptive Kalman Filter of the type used by (Zhang *et al.*) to solve the localization problem we saw under 3.3.2. However the algorithm proposed there has been developed for a linear model. However we deal with a non-linear observation equation in the localization problem. We argue that the method used in (Zhang *et al.*) ccan be extended to the non-linear case too. We use the same notation developed earlier for the Extended Kalman Filter (See Sections 3.1 and 3.2).

Prior Innovation: $z_k - h(x_k^f)$
Posterior Innovation: $z_k - h(x_k^a)$

4.1.1 Prior Innovation

As shown in the linear Kalman filter case by (Zhang *et al.*), we demonstrate that the prior innovation has zero mean and has covariance $HP_k^f H^T + R_k$ where $H = J_h(x_k^f)$.

$$\begin{aligned} h(x_k) &= h(x_k^f) + J_h(x_k^f)(x_k - x_k^f) + H.O.T. \text{ (dropped)} \\ z_k - h(x_k^f) &= z_k - h(x_k) + J_h(x_k^f)(x_k - x_k^f) \\ &= v_k + J_h(x_k^f)(x_k - x_k^f) \end{aligned}$$

At the k^{th}, x_{k-1}^a is fixed and from the forecast step, we can see that x_k^f is fixed. Therefore we conclude that $H = J_h(x_k^f)$ is a constant.

We now write

$$z_k - h(x_k^f) = v_k + H(x_k - x_k^f) \tag{4.1}$$

Taking expectation on both sides

$$E[z_k - h(x_k^f)] = E[v_k] + HE[x_k - x_k^f] \tag{4.2}$$

We now try and evaluate $E[x_k - x_k^f]$. We start from

$$f(x_{k-1}) = f(x_{k-1}^a) + J_f(x_{k-1}^a)e_{k-1} \tag{4.3}$$

where $e_{k-1} = x_{k-1} - x_{k-1}^a$ to obtain

$$x_k^f = f(x_{k-1}^a) = f(x_{k-1}) - J_f(x_{k-1}^a)e_{k-1} \tag{4.4}$$

Combining (3.1) with (4.4) we arrive at

$$x_k - x_k^f = w_{k-1} + J_f(x_{k-1}^a)e_{k-1} \tag{4.5}$$

Under EKF, we have $E[e_{k-1}] = 0$ and $E[v_k] = 0$. Applying this to (4.5) gives

$$E[z_k - h(x_k^f)] = 0 \tag{4.6}$$

We know find the covariance of the prior innovation

$$\begin{aligned} E\left[\left(z_k - h(x_k^f)\right)\left(z_k - h(x_k^f)\right)^T\right] &= E\left[\left(v_k + H(x_k - x_k^f)\right)\left(v_k + H(x_k - x_k^f)\right)^T\right] \\ &= R_k + HE\left[(x_k - x_k^f)(x_k - x_k^f)^T\right]H^T \\ &= R_k + HP_k^f H^T \end{aligned}$$

Therefore

$$E\left[\left(z_k - h(x_k^f)\right)\left(z_k - h(x_k^f)\right)^T\right] = R_k + HP_k^f H^T \tag{4.7}$$

From equations (4.6) and (4.7), we can see that the prior innovation has zero mean and variance $R_k + HP_k^f H^T$

4.1.2 Posterior Innovation

As shown in the linear Kalman filter case by (Zhang *et al.*), we demonstrate that the posterior innovation has zero mean and has covariance $R_k S^{-1} R_k$ where $S = HP_k^f H^T +$

R_k.

We begin at

$$x_k^a = x_k^f + K_k \left(z_k - h(x_k^f) \right)$$

which follows from the data assimilation step of the EKF algorithm in section 3.2

$$h(x_k^a) = h \left(x_k^f + K_k \left(z_k - h(x_k^f) \right) \right)$$

Writing the Taylor series expansion gives us

$$h(x_k^a) = h(x_k^f) + J_h(x_k^f) \left(K_k \left(z_k - h(x_k^f) \right) \right)$$

Using this in our definition of posterior innovation

$$z_k - h(x_k^a) = \left(z_k - h(x_k^f) \right) - HK_k \left(z_k - h(x_k^f) \right)$$

which simplifies further to

$$z_k - h(x_k^a) = (I - HK_k) \left(z_k - h(x_k^f) \right) \tag{4.8}$$

We can clearly see that $(I - HK_k)$ is a constant matrix. Therefore the statistics of the posterior innovation are nothing but the statistics of the prior innovation modified by a constant matrix.
From equation (4.6), we conclude that

$$E[z_k - h(x_k^a)] = 0 \tag{4.9}$$

Using (4.7) and (4.8),

$$E \left[(z_k - h(x_k^a)) (z_k - h(x_k^a))^T \right] = (I - HK_k) S (I - HK_k)^T \tag{4.10}$$

where $S = R_k + HP_k^f H^T$, the covariance of the prior innovation. Substituting for K_k from the data assimilation step of the EKF Algo (See section 3.2) in $(I - HK_k)$

$$(I - HK_k) = I - HP_k^f H^T \left(HP_k^f H^T + R_k\right)^{-1} \tag{4.11}$$

Recognizing $HP_k^f H^T = S - R_k$ and substituting in equation (4.11)

$$(I - HK_k) = I - (S - R_k)S^{-1} = R_k S^{-1} \tag{4.12}$$

Substituting (4.12) in (4.10), we finally arrive at

$$E\left[\left(z_k - h(x_k^a)\right)\left(z_k - h(x_k^a)\right)^T\right] = R_k S^{-1} R_k \tag{4.13}$$

From equations (4.9) and (4.13), we can see that the posterior innovation has zero mean and variance $R_k S^{-1} R_k$

In the next section we present the Adaptive Kalman Filter Algorithm

4.2 The Adaptive Kalman Filter Algorithm (With Inflated Noise Covariance)

We follow the same notation followed in section 3.1.

Inputs to the k^{th} run of the algorithm:

$x_{k-1}^a,\ P_{k-1},\ Q,\ R,\ h(.),\ J_h(.)$ (R and Q are not true values but initial values)

Output at the end of k^{th} run of the algorithm:

$x_k^a,\ P_k$

User defined values for the k^{th} run of the algorithm:

$\tau_{\text{Process}},\ \tau_{\text{Measurement}}$

1. Define $f(x) = x$ and calculate $J_f(.)$
2. Run the model forecast steps from 3.2
3. Calculate $S = HP_k^f H^T + R$ where $H = J_h(x_k^f)$. Also compute the prior innovation $I^- = z_k - h(x_k^f)$
4. We compute the normalized prior innovation vector (normalized by its variance) $\tilde{I^-}_i = |I_i^-|/\sqrt{S_{ii}}\ \forall i$. If $\tilde{I^-}_i > \tau_{\text{Process}}$, then $i \in Out$ where Out holds the outlier indices.
5. We assume that the outliers are caused by unknown process noise. So we inflate each diagonal element of $Q_{initial}$ by an equal amount $\Delta Q \geq 0$ such that each

diagonal element of P_k^f is inflated by ΔQ. Consequently S is inflated by $\Delta S = H(\Delta Q)H^T$ and $\tilde{I^-}_i = |I_i^-|/\sqrt{S_{ii} + \Delta S_{ii}} \leq \tau_{Process}\ \forall i$ where

$$\Delta S_{ii} = \sum_{j=1}^{n} H_{ij}^2 \Delta Q = (H(i,\ :).H(i,\ :))\ ([\Delta Q,\ \Delta Q\ ....,\ \Delta Q])^T$$

where . denotes dot product. ΔQ is the minimum possible value that satisfies

$$\Delta S_{ii} = \sum_{j=1}^{n} H_{ij}^2 \Delta Q \geq \left(|I_i^-|/\tau_{process}\right)^2 - S_{ii} \forall i \in Out$$

We therefore get $Q = Q + (\Delta Q) I_{n \times n}$

6. Use Q obtained in the previous step to recalculate P_k^f and S
7. Run the data assimilation step of the EKF algorithm from section 3.2
8. Calculate $T = RS^{-1}R$ and the posterior innovation $I = z_k - h(x_k^a)$
9. We compute the normalized posterior innovation vector (normalized by its variance) $\tilde{I}_i = |I_i|/\sqrt{T_{ii}}\ \forall i$. If $\tilde{I}_i > \tau_{\text{Measurement}}$, then $i \in MeasOut$ where $MeasOut$ holds the measurement outlier indices, indicating abnormal measurements.
10. Now, we can separate the measurement "noise" elements from the process "noise" elements. We denote $ProcOut = Out \backslash MeasOut = \{i :\ i \in Out\ and\ i \notin MeasOut\}$ as the set difference between Out and $MeasOut$.
11. If $MeasOut$ is not empty, we will reinflate Q not for all $i \in Out$ but $\forall i \in ProcOut$. We use a linear programming approach to solve the optimization problem and set $Q = Q + \Delta Q$ where ΔQ is a diagonal matrix with entries corresponding to the solution of the following optimization problem.

$$\min \sum_{i=1}^{n} \Delta Q_i$$

$$s.t\ \Delta S_{ii} = \sum_{j=1}^{n} H_{ij}^2 \Delta Q \geq \left(|I_i^-|/\tau_{Process}\right)^2 - S_{ii} \forall i \in ProcOut$$

$$\Delta Q_1 \geq 0,\ \Delta Q_2 \geq 0, ...\Delta Q_n \geq 0$$

12. As for the measurements, we "inflate" R in this way: $\forall i \in MeasOut,\ R_{ii}$ is inflated to $\lambda_i R_{ii}$. As a result, $T = RS^{-1}R$ is also inflated such that the i^{th} diagonal element is now $\lambda_i^2 T_{ii}$ and

$$\tilde{I}_i = |I_i|/\lambda_i \sqrt{T_{ii}} \leq \tau_{Measurement},\ \ i = 1, 2, ..n$$

It is relatively straightforward to compute the λ_i values by

$$\lambda_i = (|I_i|/\sqrt{T_{ii}})/\tau_{Measurement},\ \ i \in MeasOut$$

13. Using the final inflated Q and R, we recalculate the steps of the EKF under section 3.2. Optionally, the values of Q and R can be "deflated" if the process/measurement problems are only temporary.

4.3 Algorithm Performance

The algorithm presented above assumes no knowledge of the statistics of the mobility of the MS. We benchmark the performance of the algorithm by comparing it against the performance of a static positioning algorithm which also assumes no statistics of the MS mobility model and also against the performance of an EKF algorithm which has complete knowledge of the MS mobility statistics.

We assume a cellular network with equally distributed BS. We assume the MS uses TDoA information from 3 BS that form a triangle inside which the MS moves as seen in Fig. 4.1. The distance between adjacent BS is assumed to be $500m$. We set $\tau_{Process} = 1$ and $\tau_{Measurement} = 2$. We set $Q_{initial} = I$ and for $R_{initial}$ we use the gaussian TDoA model we developed in section 2.4

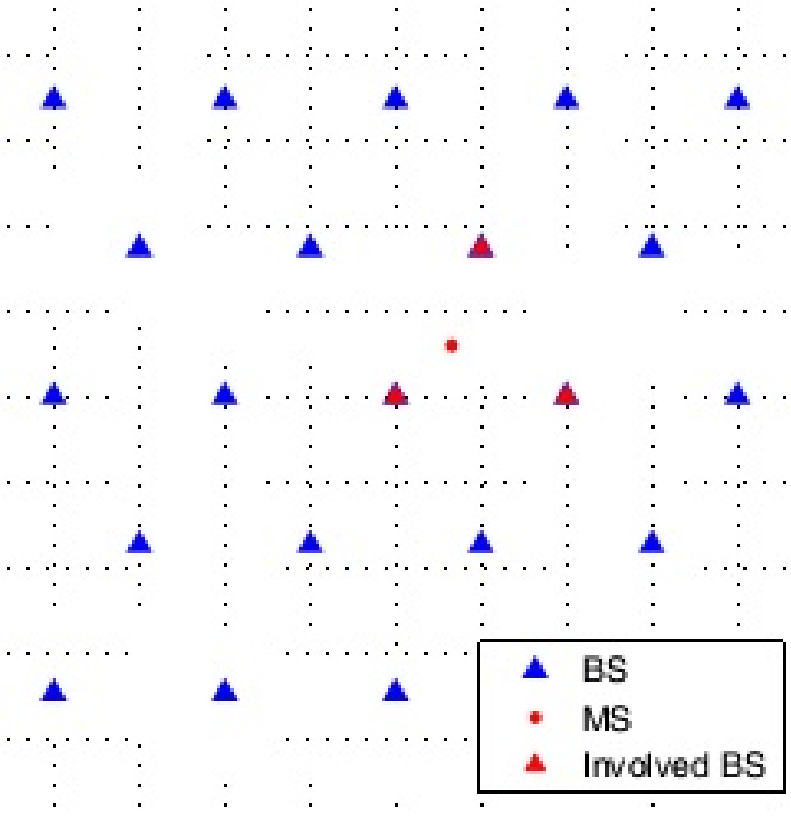

Figure 4.1: BS - MS Layout

We simulate numerous MS paths and run all three algorithms on each path. The paths simulated are a mixture of straight and curved paths. The total number of paths simulated are ~ 2000 and we measure the position error at ~ 45000 positions across all paths. We assume that all the 3 BS see the same channel scenario and that the MS "sees" the same 3 BS throughtout its entire path. Hence the ToA error due to each BS is independent and identically distributed.

Using these position errors, we build a CDF of the position errors for each algorithm for comparison. Unlike conventional Kalman filter algorithms for localization, the states do not explicitly depend on velocity. The adaptive Kalman filter algorithm developed in the above section uses just positions in its states.The same position sequence can then be assumed to have come at different sampling times accounting for different speeds. Here, we have simulated different path sequences where adjacent positions are $\sim 2m$ to $\sim 20m$ apart.

We study the performance of the algorithms under the B1 Channel Scenario, the Extended ITU Ped B Channel and the Extended ITU Veh A Channel first assuming FP is detected and second assuming SP is detected.

4.3.1 B1 Scenario: Urban Microcell

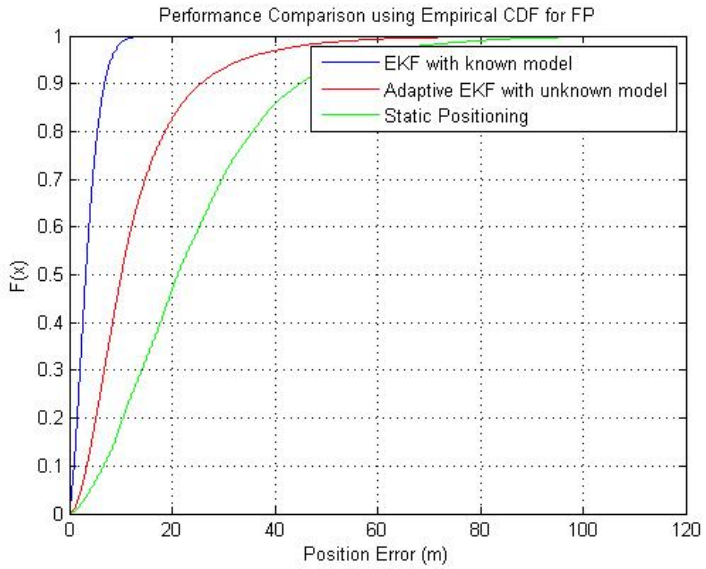

Figure 4.2: B1 Scenario: Performance comparison of algorithms under FP

We can see clearly from figures 4.2 and 4.3 that the proposed algorithm gives better

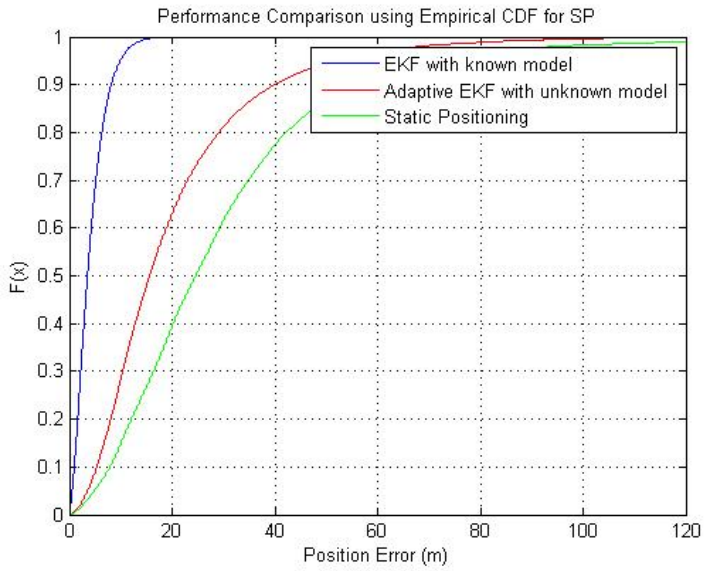

Figure 4.3: B1 Scenario: Performance comparison of algorithms under SP

results than the static positioning algoithm under the B1 channel scenario. Understandably the EKF having complete knowledge of the MS mobility statistics gives the best results.

4.3.2 Extended ITU Ped B

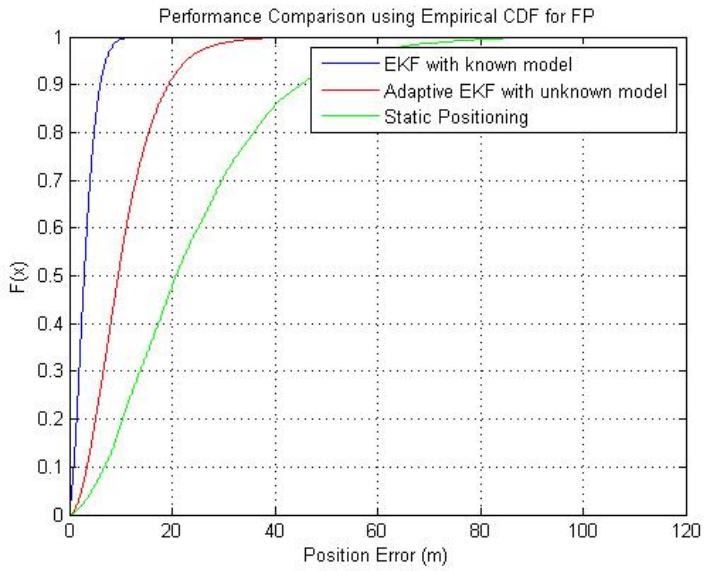

Figure 4.4: Ex ITU Ped B: Performance comparison of algorithms under FP

We can see clearly from figures 4.4 and 4.5 that the proposed algorithm gives better results than the static positioning algoithm under the the Extended ITU Ped B channel

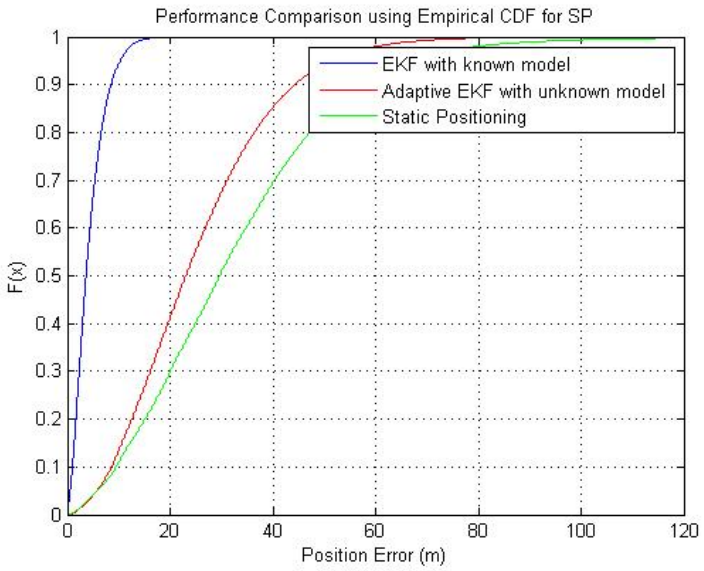

Figure 4.5: Ex ITU Ped B: Performance comparison of algorithms under SP

scenario. Understandably the EKF having complete knowledge of the MS mobility statistics gives the best results.

4.3.3 Extended ITU Veh A

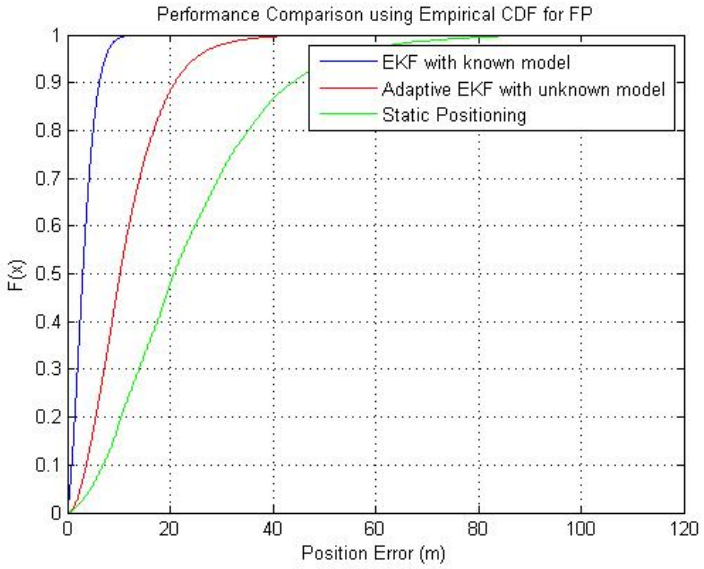

Figure 4.6: Ex ITU Veh A: Performance comparison of algorithms under FP

We can see clearly from figures 4.6 and 4.7 that the proposed algorithm gives better results than the static positioning algoithm under the Extended ITU Veh A channel scenario. Understandably the EKF having complete knowledge of the MS mobility

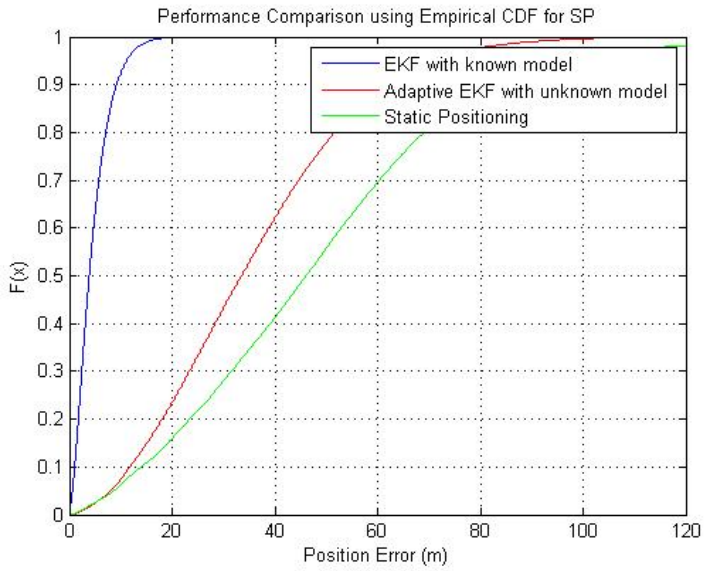

Figure 4.7: Ex ITU Veh A: Performance comparison of algorithms under SP

statistics gives the best results.

4.4 Concluding Remarks

The proposed algorithm gives better performance than the static positioning algorithm which operates under the same assumptions as our proposed algorithm. Predictably the EKF algorithm with complete knowledge of the MS mobility model does better than the proposed algorithm which has no such knowledge. However, no detailed mathematical analysis has been done on the optimality of the proposed algorithm. We have also ignored the impact of non-linearities on the EKF and have not studied the conditions under which the H.O.T. cannot be neglected. Over our simulations, the proposed algorithm gave robust performance. However further study is needed to analyse the stability of the algorithm.

The parameters like $Q_{initial}$, $R_{initial}$, $\tau_{Process}$ and $\tau_{Measurement}$ are chosen by the user and changing them may give better results depending on the situation.$\tau_{Process}$ and $\tau_{Measurement}$ can be understood as a measure of confidence in the process and measurement noise covariances respectively. Further studies can be done to identify optimal values for these parameters.

REFERENCES

1. **del Peral-Rosado, J. A.**, **J. A. López-Salcedo**, **G. Seco-Granados**, **F. Zanier**, and **M. Crisci**, Evaluation of the lte positioning capabilities under typical multipath channels. *In Advanced Satellite Multimedia Systems Conference (ASMS) and 12th Signal Processing for Space Communications Workshop (SPSC), 2012 6th*. IEEE, 2012.

2. **Gentner, C.**, **S. Sand**, and **A. Dammann**, Ofdm indoor positioning based on tdoas: Performance analysis and experimental results. *In Localization and GNSS (ICL-GNSS), 2012 International Conference on*. IEEE, 2012.

3. **Klee, U.**, **T. Gehrig**, and **J. M c Donough** (2006). Kalman filters for time delay of arrival-based source localization. *EURASIP Journal on Advances in Signal Processing*, **2006**.

4. **L. Hentila, M. K. M. N., P. Kyosti** and **M. Alatossava**, Matlab implementation of the winner phase ii channel model ver1.1 [online]. 2007.

5. **Nájar, M.** and **J. Vidal**, Kalman tracking based on tdoa for umts mobile location. *In IEEE International Symp. Personal, Indoor & Mobile Radio Communications*, volume 1. 2001.

6. **Najar, M.** and **J. Vidal**, Kalman tracking for mobile location in nlos situations. *In Personal, Indoor and Mobile Radio Communications, 2003. PIMRC 2003. 14th IEEE Proceedings on*, volume 3. IEEE, 2003.

7. **Sørensen, T. B.** and **F. Frederiksen**, Extension of the itu channel models for wideband (ofdm) systems. *In IEEE Vehicular Technology Conference*. 2005.

8. **Terejanu, G. A.**, Extended kalman filter tutorial. Department of Computer Science and Engineering, University at Buffalo, Buffalo, NY 14260, .

9. **Wang, W.**, **T. Jost**, **C. Mensing**, and **A. Dammann**, Toa and tdoa error models for nlos propagation based on outdoor to indoor channel measurement. *In Wireless Communications and Networking Conference, 2009. WCNC 2009. IEEE*. IEEE, 2009.

10. **Zhang, J.**, **G. Welch**, **G. Bishop**, and **Z. Huang** (). A two-stage kalman filtering approach for robust and real-time power systems state tracking.